Materials Today: Proceedings 93 (2023) 719–724

Contents lists available at ScienceDirect

Materials Today: Proceedings

journal homepage: www.elsevier.com/locate/matpr

Validation of a strain gauge rosette setup on a cantilever specimen: Application to a calibration bench for residual stresses

Marco Beghini, Tommaso Grossi *, Ciro Santus

Dipartimento di Ingegneria Civile e Industriale, Università di Pisa, Largo Lucio Lazzarino, Pisa 56122, Italy

ARTICLE INFO

Article history:
Available online 1 June 2023

Keywords:
Residual stress
Hole drilling
X-Ray Diffraction
Calibration Bench
Systematic errors
Shot peening

ABSTRACT

It is commonly known that the most difficult part of measuring residual stresses through diffraction or relaxation methods is the high sensitivity of the results to input errors, such as noise in the strain data. Then, quantifying and minimizing stress uncertainties is at least as important as the residual stress results themselves. Results are often validated by leveraging different measurement techniques, although each method is somehow specialized at detecting residual stresses at different locations and length scales. This leads to a fundamental lack of ground truth data and an inherent difficulty in detecting biases.

The authors have introduced a calibration bench that facilitates the application of a well-known bending stress distribution on a specimen while conducting residual stress measurements using either the Hole-Drilling Method (HDM) or X-ray Diffraction (XRD). By leveraging Bueckner's superposition principle, the bench allows for determination of both the residual stress distribution and the reference stress distribution through a single experimental setup. This approach not only enables direct evaluation of accuracy but also identification of any procedural systematic errors, as the reference stress distribution is known with a high degree of certainty.

In this work, a detailed characterization of the stress and strain fields generated by the externally applied load was pursued. Then, the calibration bench was used to perform a validated characterization of residual stresses produced by two shot peening treatments, through both XRD and HDM. Additionally, both techniques were employed to verify the recognized bending stresses, thereby validating the findings of the residual stress measurements.

Selection and peer-review under responsibility of the scientific committee of the 38th Danubia- Adria Symposium on Advances in Experimental Mechanics.

1. Introduction

Residual stresses in mechanical components can significantly increase the risk of fatigue failure, corrosion, and distortion. These stresses can be caused by a variety of factors, including manufacturing processes, and can lead to reduced component lifespan and increased maintenance costs [1–3]. Among various measurement techniques [4–6], the Hole Drilling Method (HDM) [7–10] is a popular and cost-effective way to measure residual stresses. Standardization for this method is provided by ASTM E837 procedure [11], and tools like the MTS3000-Restan by SINT Technology are commonly used to carry out measurements. However, HDM has limitations [12], especially near the surface [13], where stress values depend on just a few measurement points, and errors in the zero-depth datum can affect accuracy. Additionally, HDM becomes less effective at greater depths. To supplement HDM, X-Ray Diffraction (XRD) [14] is used to identify residual stresses near the surface [15]. Electropolishing can remove layers of material to investigate deeper stresses. However, the accuracy of XRD measurements depends on the material's crystallographic properties and on the diffraction peaks identification strategy, requiring a careful setup assessment.

To address these issues, the authors developed a calibration bench, described in references [16–18]. It applies a predetermined distribution of bending stress to a test specimen while at the same time using XRD or HDM to measure residual stress. By comparing the identified bending stress distribution with the known distribution, this calibration apparatus can directly confirm the validity of residual stress measurements. Differences between the two distributions can also highlight potential issues with the instrument

* Corresponding author.
E-mail address: tommaso.grossi@phd.unipi.it (T. Grossi).

https://doi.org/10.1016/j.matpr.2023.05.505

Selection and peer-review under responsibility of the scientific committee of the 38th Danubia- Adria Symposium on Advances in Experimental Mechanics.

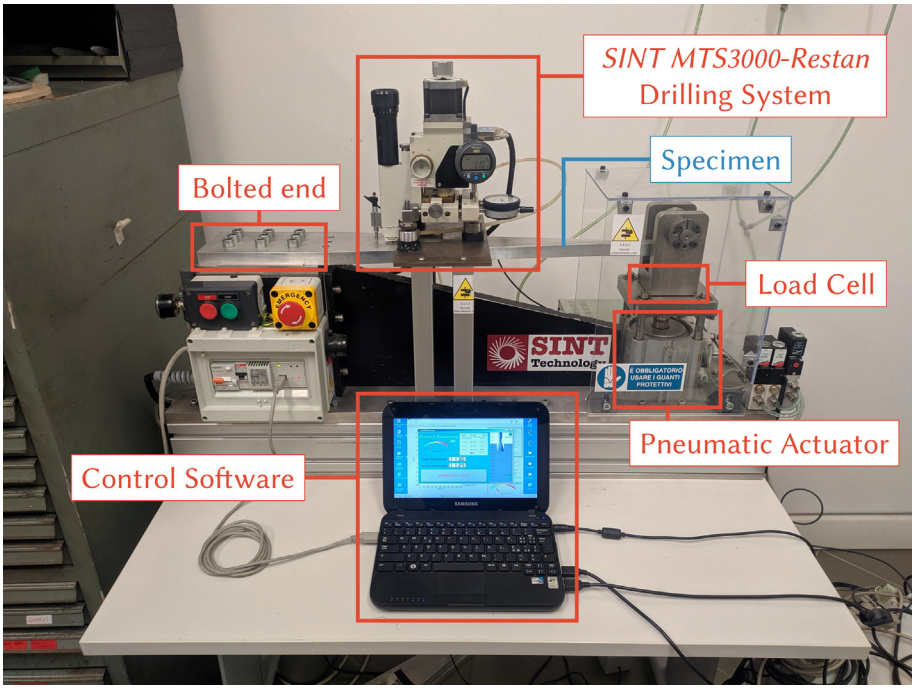

Fig. 1. The calibration bench: description of its components.

setup, calibration, or material properties. Fig. 1 shows the bench, and additional details can be found in [17].

To accurately determine the bending stress distribution, two measurements must be taken, one when the sample is unloaded and the other when it is loaded. Assuming linear elasticity, the difference between the two measurements reflects the impact of bending alone, while the unloaded measurement only accounts for actual residual stresses.

For the bending stress distribution to be considered ground truth data, it must be precisely known, surpassing the typical accuracy of residual stress measurements. In this study, a combination of beam theory, non-linear FEM modeling, and experimental strain gauge testing was employed to accurately characterize the applied stress distribution. Having demonstrated that the uncertainty of the bending distribution is insignificant with respect to residual stress analyses, the calibration bench was utilized to confirm XRD and HDM measurements on a 7075-aluminum specimen, shown in Fig. 2, that underwent two shot-peening treatments. The standard HDM experimental setting with strain gauge rosettes was employed, although the bench is agnostic to the specific strain measuring technique.

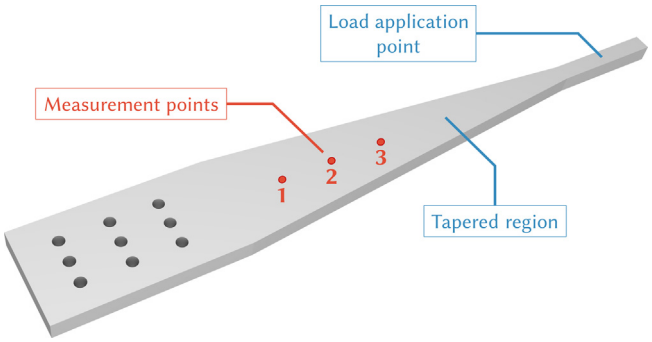

Fig. 2. 3D model of the 110 × 440 mm aluminum specimen, manufactured from a 20 mm plate. The load application point and the measurement positions are highlighted.

2. Materials and methodology

2.1. The bench

The system is depicted in Fig. 1 and features a pneumatic cylinder that generates a vertical deflection of about 40 mm on the unsupported end of a cantilever beam. A load cell is positioned between the actuator and the specimen's contact point, to measure the applied load. The residual stress analysis is conducted on the tapered midsection of the beam. To ensure uniform bending stresses on both the top and bottom surfaces of the tapered area, the load application point is placed where the geometrical extensions of the two lateral surfaces intersect. The specimen can be varied by adjusting its thickness to attain the desired bending stress levels, which should anyway be consistent with the actuator's rated load.

No system components need to be disassembled to apply or remove the bending load. Strain measurements reflect the influence of residual stresses on the specimen when no load is present. In contrast, when the bending load is applied, the strain measurements represent the combined impact of residual stresses and the superimposed bending distribution. Under the assumption of linearity, the difference between the strain measurements in both configurations provides a precise evaluation of the bending distribution's effect, allowing for the identification and correction of potential biases that may arise during the identification process, and validating bias correction methods. Further details on the experimental setup are available in [17].

2.2. FEM model

To establish a reference system, the x-axis was aligned with the longitudinal axis of the specimen, the z-axis was oriented outward from the upper surface of the specimen, and the y-axis was determined accordingly, as shown in Fig. 3. A finite element model of the specimen was created utilizing ANSYS, as depicted in Fig. 4. The model utilized second-order hexahedral elements (SOLID186)

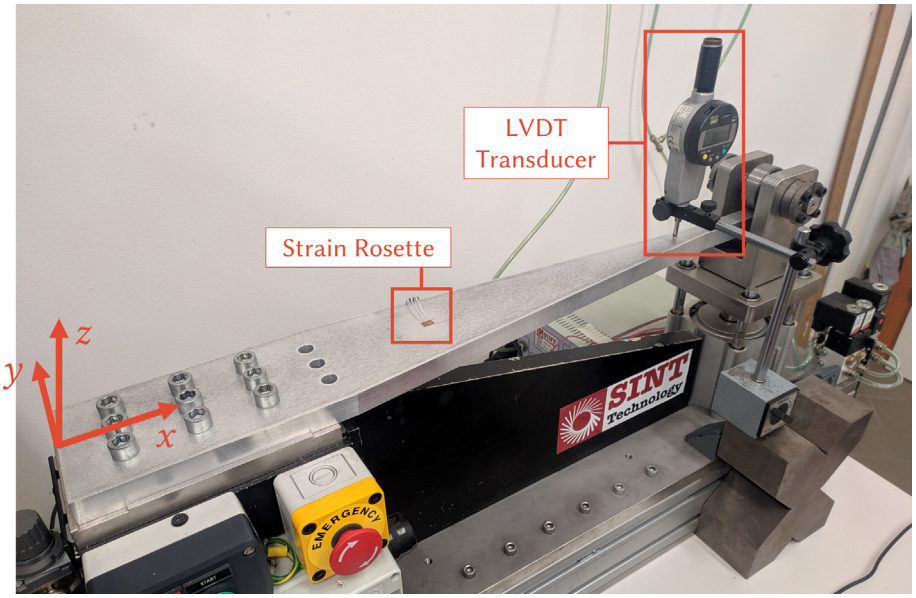

Fig. 3. Reference system, LVDT vertical deflection measurements and strain gauge rosette positioning.

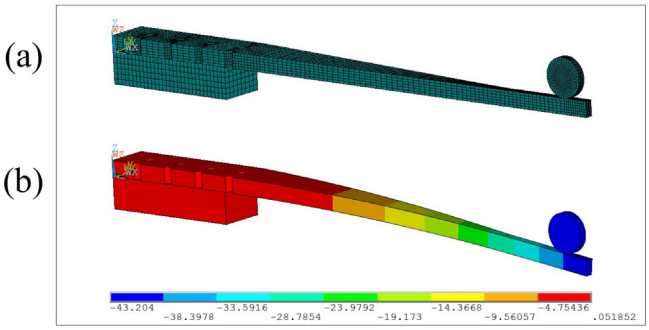

Fig. 4. 3D FEM model of the bench.

and exploited geometrical symmetry along the *xz* plane. Contact elements were utilized to model the load application device interface and bolted constraint. Non-linear geometry effects were considered, and bolt preloads were applied before the analysis. The 40 mm vertical deflection was applied in 100 steps, and the globally applied force was recorded at each step.

2.3. Experimental deflection tests

The deflections in the tapered region of the specimen were measured using a linear variable differential transformer (LVDT), as shown in Fig. 3. The uniformly curved tapered region observed in the deflection measurements aligns with the predictions of classical beam theory, which was confirmed by fitting the deflection measurements to a quadratic formula, with insignificant residuals. Negligible shear deformation effects on the tapered region's curvature were also observed.

The FEM model's elastic constants can be arbitrarily set as the maximum displacement is fixed and does not depend on these constants. However, discrepancies between the modeled and experimental deflections arise from the actual compliance of the bolted end and the actual displacement imposed by the piston. To reconcile this, the end-displacement applied to the FEM model was adjusted until the modeled and experimental curvatures matched. This process is independent of any errors in elastic constants or applied load. It has been confirmed through a sensitivity analysis that the accuracy of the experimental curvature is 0.1%, which is anticipated to be at least as accurate as the FEM outcomes.

2.4. Strain gauge measurements

A Type-B strain gauge rosette (HBM RY61-1.5/120 K) was attached to the specimen in the tapered region, as shown in Fig. 3; it was later reused to carry out a HDM measurement on the same point. By combining the readings from the rosette with the strain characterization of the last section, the elastic constants of the material and the rosette gauge factors were validated. The expected positive principal strain from the rosette should match the results of the tuned FEM model within an acceptable gauge factor tolerance, to validate the strain gauge setup. Additionally, the orientation of the principal strains measured in relation to the longitudinal axis of the specimen was established. The Poisson ratio of the material and the gauge factors were validated according to the procedure presented in [17].

The load cell was calibrated under an MTS hydraulic uniaxial machine with a class 0.5 load sensor. The measured bending load was then compared with the corresponding constraint load in the tuned FEM model to identify differences, mainly attributed to errors in the nominal value of the material Young's modulus, which were then corrected. Furthermore, the load cell readings allowed for the determination of the stress fields in the tapered region using beam theory, which should correspond to the accurately known strain fields through the correct Young's modulus.

2.5. Residual stress measurements

The specimen was subjected to two shot-peening treatments, namely AZB425 and CEB120, on both of its sides by Peen Service Srl, and specific details on the shot-peening parameters can be found in reference [16]. To measure the effects of the treatments, three points were marked on each side of the specimen (as shown in Fig. 2). Surface XRD measurements were conducted on all three points, whereas points 1 and 2 underwent HDM analysis. On the other hand, XRD and electrochemical layer removal methods were employed to analyze the stress profile at point 3. In both loaded

and unloaded conditions, measurements were taken to determine both residual and bending stresses.

An MTS3000-Restan system by SINT Technology was utilized to conduct the HDM measurements, while a GNR SpiderX Edge diffractometer was used to perform the XRD measurements (see Fig. 5). A final depth of 1.0 mm was reached through 100 drill steps. The external load was applied and removed during each drilling step. On the other hand, XRD measurements were carried out by following the $\sin^2\psi$ method, by probing the lattice spacing of {3 1 1} planes with a chrome anode.

3. Results

3.1. Characterizations of bending deflections and stresses

Fig. 6 shows the vertical deflections measured along the tapered region, along with the corresponding FEM results, and a quadratic interpolation. The small residuals suggest that the curvature is constant. While there were some discrepancies between the experimental and modeled vertical deflections due to the compliance of the specimen at the bolted end, the latter does not affect the curvature or strains in the tapered region. The experimental and simulated curvatures matched when the applied displacement in the FEM model was adjusted at 38.75 mm, which is reasonable considering the bolted end compliance and the chain of free-plays between the piston rod and load application point.

The maximum principal strain measured by the strain gauges was 2362 με, whereas the FEM model yielded a value of 2347 με at the same point. Despite the difference being less than 1%, the strain readings were adjusted by scaling to account for it. Additionally, a 0.25-degrees misalignment was observed between the rosette grids and the longitudinal axis of the specimen.

Using beam theory, the longitudinal normal stress was computed to be 164 MPa by considering the recorded load of 2357 N. The material's (secant) Young's modulus was determined to be 70.0 GPa, and its precision is mainly dependent on the uncertainties in load measurements, which are estimated to be in the range of one percent. Moreover, the Poisson ratio was evaluated to be 0.31.

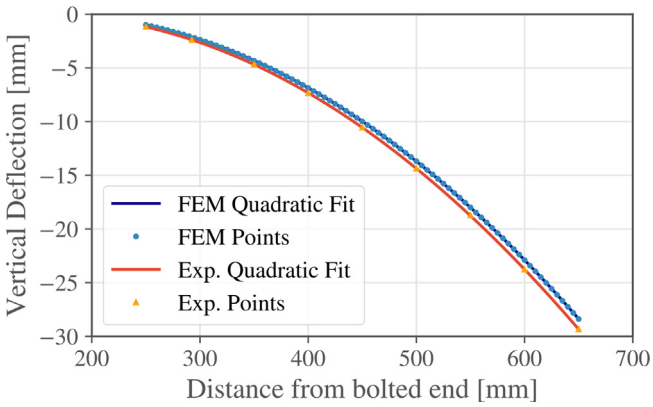

Fig. 6. Vertical deflections (FEM model and experimental tests).

3.2. Residual stress characterization and simultaneous bending stress identification

The bending stress distribution validation data for the identified stresses using XRD are shown in Fig. 7. Each graph shows a stress tensor component obtained from 3 measurements taken at different angles. The bending stress distributions identified using HDM are presented in Fig. 8, where the procedure outlined in [17]–[19] was followed to determine the stresses. Additionally, Fig. 9 compares the residual stress fields obtained from HDM measurements at points 1 and 2 with XRD depth profiling carried out at point 3.

4. Discussion

The FEM model and experimental deflection measurements showed remarkable correlation, especially in terms of curvature.

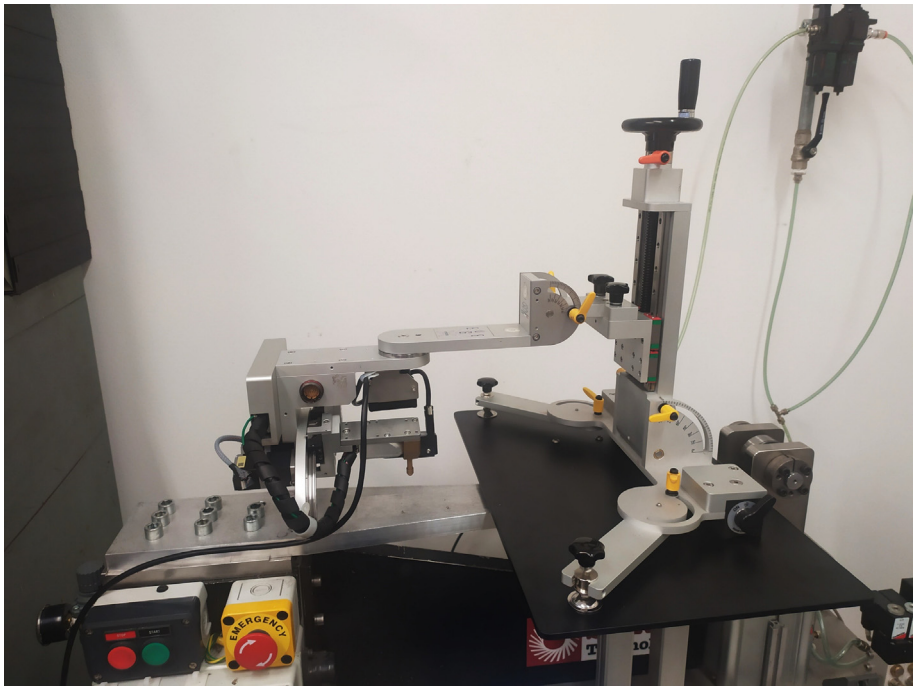

Fig. 5. GNR SpiderX Edge diffractometer, positioned on the bench and ready to measure.

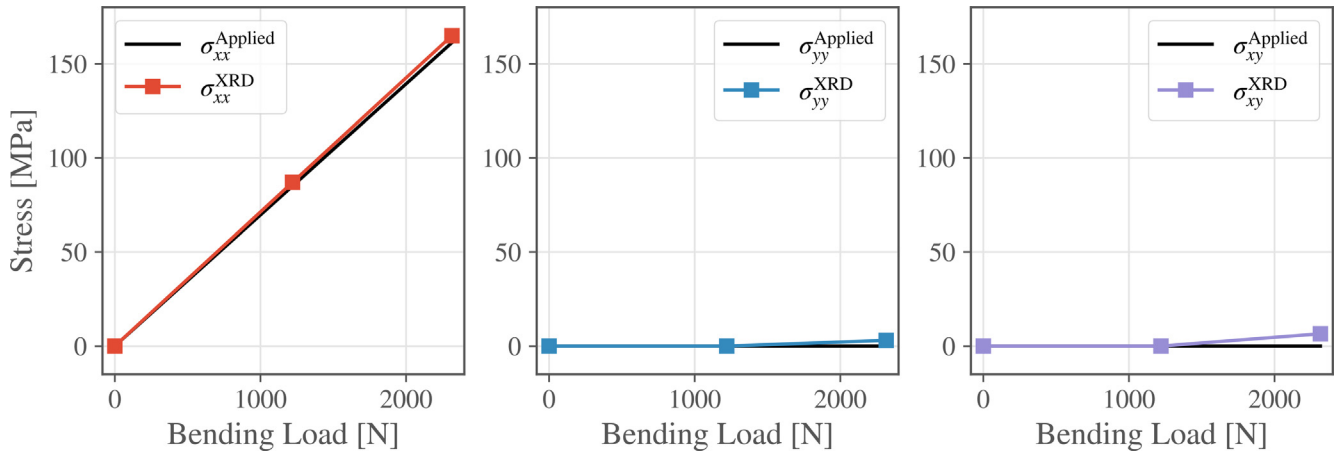

Fig. 7. XRD surface identification of the applied stress state.

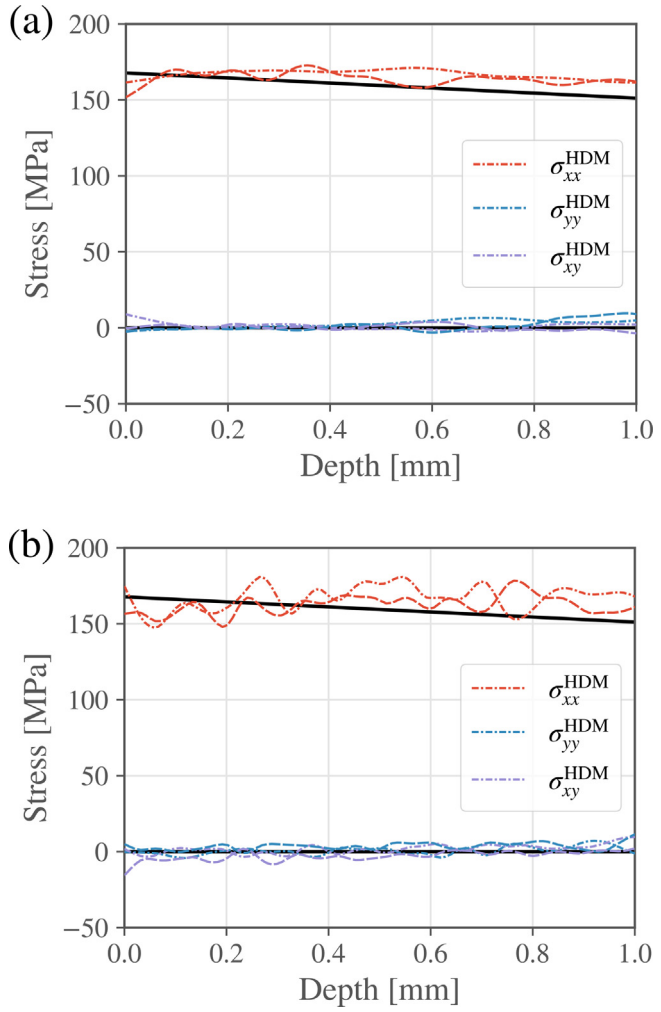

Fig. 8. HDM identification of the applied stress distribution. Reference values are shown as black solid lines, the only non-null curve being σ_{xx}. (a) AZB425 side; (b) CEB120 side.

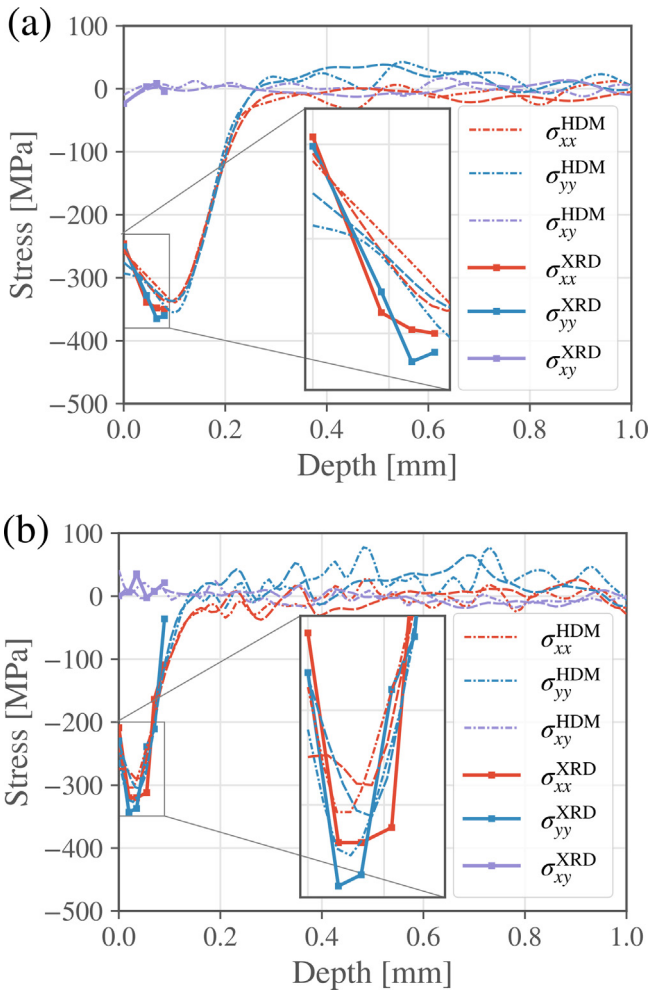

Fig. 9. Measured residual stress distributions: HDM on points 1–2 and XRD with layer removal on point 3. (a) AZB425. (b) CEB120.

Extracting the compliance of the bolted constraint from the data could improve the correlation, although it would be irrelevant for bending strain identification. The calibration bench is advantageous for checking elastic constants, since the residual stress results obtained with relaxation methods depend on them. However, it should not be seen as a substitute for proper testing of elastic properties, though decent accuracies can be achieved anyway.

The instrumentation setup was correctly executed, as evidenced by the accurate XRD surface measurements of stress fields produced by bending load shown in Fig. 7. The results were slightly less precise for σ_{xy} at high loads, which is expected since they

are computed from a combination of XRD measurements at all three orientations (so absolute errors are summed). HDM measurements successfully captured bending stress distribution throughout the hole depth, as seen in Fig. 8, with a maximum absolute error of ± 25 MPa for the highest stress component σ_{xx}, which is consistent with the current state of the art [11].

HDM residual stress profiles for shot peening treatments in Fig. 9 are consistent with the maximum ± 25 MPa error seen in bending measurements, while XRD stress profiles closely follow the trend of HDM curves with up to 50 MPa discrepancy at a given depth. The accuracy of the results was likely impacted by uncertainties in the planarity of the etched surface and inaccuracies in measuring the etching depth. Despite this, the accuracy remains reasonable for engineering purposes. Further research will be conducted on the grain size of the specimen material and potential material texturing.

5. Conclusions

A calibration system has been introduced, which allows for accurate generation of bending stress distributions in a specimen, as well as verification of strain gauge readings independently from uncertainties related to the material's elastic properties and external load measurements. The calibration system provides a means of validating the experimental setup both prior to and during residual stress measurements using XRD and HDM. Inadequacies such as inadequate texture or insufficient grain statistics in the material, as well as issues with strain gauge bonding, would lead to significant errors in determining the bending distribution and would be detected. The bench's versatility in accommodating various materials and geometries makes it useful for exploring residual stresses produced by novel surface treatments, as the validation phase improves measurement confidence.

As an example, the bending stress distribution was accurately characterized for a 7075-aluminum specimen, then the results were leveraged to perform a validated characterization of two shot peening treatments. The consistency of the identified bending distributions with their known values is a valuable confirmation of the measurement setup and allows one to estimate the reached accuracy level.

CRediT authorship contribution statement

Marco Beghini: Conceptualization, Methodology, Investigation, Writing – review & editing, Supervision, Funding acquisition. **Tommaso Grossi:** Conceptualization, Methodology, Software, Validation, Formal analysis, Investigation, Data curation, Writing – original draft. **Ciro Santus:** Conceptualization, Methodology, Investigation, Writing – review & editing, Supervision, Funding acquisition.

Data availability

Data will be made available on request.

Declaration of Competing Interest

The authors declare that they have no known competing financial interests or personal relationships that could have appeared to influence the work reported in this paper.

Acknowledgements

The authors would like to thank Alessio Benincasa, Enrico Boccini, Simone Gulisano, and Emilio Valentini of SINT Technology srl (Calenzano, Italy) for their contributions to the design of the calibration bench. They also extend thanks to Luigi Pisani, Luca Seralessandri, and Alessandro Torboli of GNR srl (Agrate Conturbia, Italy) for their support with X-Ray Diffraction measurements. Michele Bandini of Peen Service srl (Bologna, Italy) performed the shot peening treatments and is gratefully acknowledged.

References

[1] H. Alzyod, P. Ficzere, "Failures/Breakdowns Due to Residual Stresses in the Vehicle Industry," *Int. J. Traffic Transp. Eng.* vol. 12 (2) 2022, Accessed: May 12, 2023. [Online]. Available: https://trid.trb.org/view/1946753.
[2] F. Kümmel, A. Magnier, T. Wu, T. Niendorf, H.W. Höppel, Residual stresses in ultrafine-grained laminated metal composites analyzed by X-ray diffraction and the hole-drilling method, Adv. Eng. Mater. 24 (9) (2022) 2200274, https://doi.org/10.1002/adem.202200274.
[3] H. Soyama, C. Kuji, T. Kuriyagawa, C.R. Chighizola, M.R. Hill, Optimization of residual stress measurement conditions for a 2D method using X-ray diffraction and its application for stainless steel treated by laser cavitation peening, Materials 14 (11) (May 2021) 2772, https://doi.org/10.3390/ma14112772.
[4] H. Alzyod, P. Ficzere, "Using the Photostress Method to Determine the Residual Stresses," *Int. J. Eng. Manag. Sci.* vol. 7 (2) (2022).
[5] A. Greco, E. Sgambitterra, F. Furgiuele, A new methodology for measuring residual stress using a modified Berkovich nano-indenter, Int. J. Mech. Sci. 207 (Oct. 2021), https://doi.org/10.1016/j.ijmecsci.2021.106662.
[6] C.H. Gur, Review of residual stress measurement by magnetic Barkhausen noise technique, Mater. Perform. Charact. 7 (4) (2018) 504–525.
[7] E.M. Beaney, Accurate measurement of residual stress on any steel using the centre hole method, Strain 12 (3) (1976) 99–106, https://doi.org/10.1111/j.1475-1305.1976.tb00194.x.
[8] G.S. Schajer, Application of finite element calculations to residual stress measurements, J. Eng. Mater. Technol. 103 (2) (Apr. 1981) 157–163, https://doi.org/10.1115/1.3224988.
[9] G.S. Schajer, Measurement of non-uniform residual stresses using the hole-drilling method. Part I—Stress calculation procedures, J. Eng. Mater. Technol. 110 (4) (Oct. 1988) 338–343, https://doi.org/10.1115/1.3226059.
[10] G.S. Schajer, Measurement of non-uniform residual stresses using the hole-drilling method. Part II—Practical application of the integral method, J. Eng. Mater. Technol. 110 (4) (Oct. 1988) 344–349, https://doi.org/10.1115/1.3226060.
[11] American Society for Testing and Materials, "Test Method for Determining Residual Stresses by the Hole-Drilling Strain-Gage Method," *West Conshohocken PA*, 2020, doi: 10.1520/E0837-20.
[12] M. Beghini, T. Grossi, M.B. Prime, C. Santus, Ill-Posedness and the bias-variance tradeoff in residual stress measurement inverse solutions, Exp. Mech. 63 (3) (Mar. 2023) 495–516, https://doi.org/10.1007/s11340-022-00928-5.
[13] C.R. Chighizola et al., Intermethod comparison and evaluation of measured near surface residual stress in milled aluminum, Exp. Mech. 61 (8) (Oct. 2021) 1309–1322, https://doi.org/10.1007/s11340-021-00734-5.
[14] I.C. Noyan, J.B. Cohen, Residual stress: measurement by diffraction and interpretation, Springer, 2013.
[15] M.E. Turan, F. Aydin, Y. Sun, M. Cetin, Residual stress measurement by strain gauge and X-ray diffraction method in different shaped rails, Eng. Fail. Anal. 96 (Feb. 2019) 525–529, https://doi.org/10.1016/j.engfailanal.2018.10.016.
[16] E. Valentini, M. Beghini, L. Bertini, C. Santus, M. Benedetti, Procedure to perform a validated incremental hole drilling measurement: Application to shot peening residual stresses: Validated IHD measurement test rig, Strain 47 (Jun. 2011) e605–e618, https://doi.org/10.1111/j.1475-1305.2009.00664.x.
[17] M. Beghini, T. Grossi, C. Santus, E. Valentini, "A calibration bench to validate systematic error compensation strategies in hole drilling measurements," in *ICRS 11–11th International Conference on Residual Stresses*, 2022. doi: https://doi.org/10.36227/techrxiv.20347788.v1.
[18] M. Beghini, T. Grossi, C. Santus, L. Seralessandri, S. Gulisano, Residual stress measurements on a deep rolled aluminum specimen through X-Ray Diffraction and Hole-Drilling, validated on a calibration bench, IOP Conf. Ser. Mater. Sci. Eng. 1275 (1) (Feb. 2023), https://doi.org/10.1088/1757-899X/1275/1/012036.
[19] M. Beghini, T. Grossi, C. Santus, A. Torboli, A. Benincasa, M. Bandini, "X-Ray Diffraction and Hole-Drilling residual stress measurements of shot peening treatments validated on a calibration bench," presented at the ICSP14, Milan, Italy, 2022. [Online]. Available: https://www.shotpeener.com/library/detail.php?anc=2022101.